ChemComm

COMMUNICATION

View Article Online
View Journal | View Issue

Cite this: *Chem. Commun.*, 2017, 53, 7804

Received 11th May 2017,
Accepted 19th June 2017

DOI: 10.1039/c7cc03673f

rsc.li/chemcomm

Controllable porosity conversion of metal-organic frameworks composed of natural ingredients for drug delivery†

Jiang Liu,‡[ab] Tian-Yi Bao,‡[c] Xi-Ya Yang,[a] Pei-Pei Zhu,[a] Lian-He Wu,[d] Jing-Quan Sha,*[ad] Lei Zhang,[b] Long-Zhang Dong,[b] Xue-Li Cao[b] and Ya-Qian Lan*[b]

Two extremely rare β-cyclodextrin (β-CD) supported metal-organic frameworks (MOFs), CD-MOF-1 and CD-MOF-2, were induced to crystallize for the first time through a template-induced approach. The targeted CD-MOFs were employed to perform controlled drug delivery and cytotoxicity assays that confirmed their favourable biological potential of being used as drug carriers.

Metal-organic frameworks (MOFs) constructed with mono-/polymetallic centres and organic linkers in the past few decades have been developed as a most conspicuous area due to their controllable structures and porosities that can be used in gas storage, separation, sensing and catalysis.[1–3] Another prominent trait is that the crystalline nature of MOFs is conducive to monitoring the reaction processes of solid-state chemistry, and then offers a valuable insight into the structure–property relationship.[4] Therefore, it is hoped that these noteworthy advantages can be further extended to significant domains which are tightly related to living systems, such as biological and pharmacological investigations.[5–9] Starting from the security criterion of an organism, however, the existing MOFs seem to be ill suited to be an ideal object, since the fabricated organic struts are commonly derived from non-renewable and toxic petrochemical sources.[10] In this sense, exploring desirable MOFs composed of naturally innoxious components to overcome the issue of toxicity will be a promising strategy.

Being one kind of semi-natural product, the nontoxic cyclodextrins (CDs) obtained from starch *via* a simple enzymatic conversion are extremely appropriate for extensive applications and large-scale industrial production.[11–13] These cyclic oligosaccharides commonly consist of six, seven or eight D-glucopyranoside units linked together by α-1,4-glycosidic bonds (termed as α-, β- or γ-CDs) and display the omnipresent –OCCO– binding motifs on both their primary and secondary faces (Scheme S1, ESI†), suggesting the formation of extended architectures with metal cations.[10,14–19] Such kinds of renewable and wholesome ingredients with an amphiphilic cavity serve as building blocks to construct porous MOFs that may hold promise for biological and therapeutic applications.[20,21] Nevertheless, it is an undeniable fact that so far the CD supported MOFs (CD-MOFs) are still reported scarcely, since the inherent asymmetry of the building blocks is not amenable to crystallization in the form of highly porous frameworks. Although some significant advances toward carbon dioxide (CO_2) capture, multicomponent separation and photocatalysis have recently been achieved using "green" porous CD-MOFs reliant on C_8-symmetric γ-CDs,[14,17,22] the exploration of β-CDs remains a nascent field (Scheme S1, ESI†), as their C_7-asymmetric arrangement means a lower crystallinity.[15] Fortunately, the in-depth quantitative studies in the past few decades into the inclusion complexation and host–guest chemistry of CDs can offer us more theoretical foundations[23–40] to establish possible porous CD-MOFs through a reasonable choice of guest molecules/template agents to exert an influence on the spatial arrangement of CDs during the reaction process.[41,42]

Herein, we report two helical microporous Cs-CD-MOFs, CD-MOF-**1** and CD-MOF-**2** (Table S1, ESI†), constructed by β-CD as building blocks as well as cesium metal salts, with the help of 1,2,3-triazole-4,5-dicarboxylic acid (H_3tzdc), methyl benzene sulfonic acid (TsOH) or an ibuprofen molecule (IBU) as selective template agents. To the best of our knowledge, this kind of template-induced approach was employed for the first time for the synthesis of β-CD based MOFs, and this novel synthetic strategy indicated that the size effect of the selected template agents has implications on the porosity and crystallization of the resulting CD-MOFs. Additionally, these two

[a] *Key Laboratory of Inorganic Chemistry in Universities of Shandong, Department of Chemistry and Chemical Engineering, Jining University, Qufu, Shandong, 273155, P. R. China. E-mail: shajq2002@126.com*
[b] *Jiangsu Key Laboratory of Biofunctional Materials, College of Chemistry and Materials Science, Nanjing Normal University, Nanjing 210023, P. R. China. E-mail: yqlan@njnu.edu.cn*
[c] *The Second Hospital of Jilin University, Changchun, 130041, P. R. China*
[d] *The Provincial Key Laboratory of Biological Medicine Formulation, School of Pharmacy, Jiamusi University, Heilongjiang, Jiamusi, 154007, P. R. China*

† Electronic supplementary information (ESI) available. CCDC 1404895 and 1407798. For ESI and crystallographic data in CIF or other electronic formats see DOI: 10.1039/c7cc03673f

‡ These authors contribute equally to this work.

CD-MOFs have been confirmed as biocompatible drug carriers by cytotoxicity assays that exhibit a high delivery capacity for anti-cancer drug molecules, and the size and shape of their pores have significant effects on the loading capacity and the release speed of the drugs, which may be useful for some specific requirements of pharmaceuticals.

The CD-MOFs involved in this work were solvothermally obtained as single crystals by using the same protocol (see the ESI† for details) except for the addition of different template agents (H_3tzdc, TsOH or IBU). When the appointed templates with different sizes, H_3tzdc (<5 Å), TsOH and ibuprofen (>6 Å), were used they directly resulted in different channel arrays of CDs during the reaction process (Scheme 1). A large number of parallel experiments (Table S2, ESI†) suggest that the existence and unit length of the selected template agents overall play important roles in the isolation and crystallization of CD-MOF-**1** and CD-MOF-**2** (Fig. S1, ESI†), which will be described in detail later. As for other factors, such as the solvent, temperature and the ratio of the metal salt to β-CD, compared with the impact of the template agents, they do not seem to be as essential for the preparation of the target CD-MOFs. The purity of both CD-MOFs was confirmed by powder X-ray diffraction patterns (Fig. S2, ESI†).

Single crystal X-ray diffraction analysis reveals that CD-MOF-**1** crystallizes in the monoclinic *P*21 space group and the asymmetric unit contains only one Cs^+ ion and one β-CD molecule. The six coordination sites of a strongly distorted pentagonal pyramid geometry (Table S3, ESI†) of the individual Cs^+ ion are shared by four contiguous β-CD molecules (Fig. 1a), wherein the five O atoms on the bottom surface originate from one primary hydroxyl (O15), two secondary hydroxyls (O8 and O9) and two glycosidic ring O (O1 and O11) atoms of three β-CD molecules located on the same plane, while the apical position is occupied by one primary hydroxyl (O30) from the residual β-CD molecule (Fig. 1b). Conversely, each crystallographically independent β-CD molecule is connected to four Cs^+ ions by donating its secondary hydroxyl, primary hydroxyl and the ring oxygen atom of (**a**, **d**, **e** and **f**) α-1,4-linked glucopyranosyl (Fig. 1c). In the presence of a 2_1 screw axis, the waveform distribution of the Cs^+ ion accompanied by three neighbouring β-CD molecules along the *b* direction results in a one-dimensional (1D) chain, as shown in Fig. 1d. The communication between the adjacent chains realized by the opposite Cs–O (O30) bonds of the metal sites situated at the crest and the trough of waves further results in a ladder-shaped two-dimensional (2D) layer, which ultimately determines an asymmetric stacking between the layers triggered by supramolecular interaction. It should be noted that the inherent cavities of β-CD molecules within CD-MOF-**1** were changed into atypical channels as a result of the occurrence of the "malposition" stacking effect (Fig. S3, ESI† and Fig. 1e). Furthermore, the guest-accessible volume of CD-MOF-**1** accounted for 19.5% (589.2 $Å^3$) of the unit-cell volume (3027 $Å^3$), estimated using the PLATON program. We believe that the aperture characteristic of such edible CD-MOFs can be considered as a reliable carrier for loading specific small molecules.

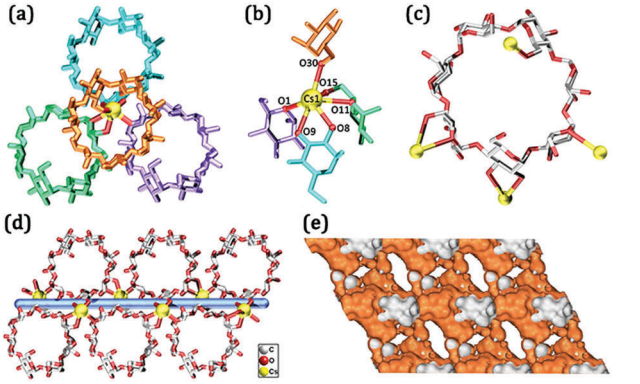

Fig. 1 (a) Stick view of four neighboring β-CD molecules coordinated to the Cs^+ ion. (b) Coordination sphere of individual Cs^+ ion. (c) View of four Cs^+ ions directly linked with each independent β-CD molecule. (d) Top view of the one-dimensional (1D) chain constructed by the alternating arrangement of Cs^+ ions along the *b* direction. (e) Representation of accessible voids of CD-MOF-**1** viewed down the crystallographic *b* axis. Color code: Cs, yellow; O, red; and C, grey. Hydrogen atoms have been eliminated for clarity.

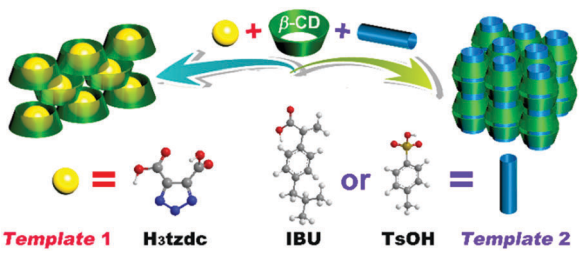

Scheme 1 Schematic view of the structural formation of CD-MOF-**1** (left) and CD-MOF-**2** (right) by using different templates in the reaction process.

The framework of CD-MOF-**2** crystallizes in the monoclinic *C*2 space group, and the asymmetric unit contains one and a half crystallographically independent Cs^+ ions and one β-CD molecule. The ten coordination sites of the staggered dodecahedron geometry of the individual Cs1 ion tightly immobilize three pairs of β-CD molecules (Table S3 and Fig. S4a, ESI†), each of which stacks in a primary face to primary face/secondary face to secondary face (PTP/STS) manner, horizontally along the diagonals of the triangle, resulting in a maximum bareness of the intrinsic cavity of the β-CD molecule (Fig. 2a). The Cs2 ion, in contrast, exhibits a similar staggered dodecahedron geometry (Table S3 and Fig. S4b, ESI†) and identical high coordination numbers to link with two pairs of such β-CD molecules, with exactly the reverse packing arrangement (PTP and STS), as shown in Fig. 2b. The two adjacent Cs2 sites encompassing the *C*2 rotation axis link with each other through double secondary hydroxyl (μ-OH) bridges. It is worth mentioning that the versatile essence of the β-CD molecule in CD-MOF-**2** allows it to concurrently bind seven metal ions, including three Cs1 and four Cs2 sites, by employing its glycosidic ring O (O1, O11 and O21) atoms, primary hydroxyl (O5, O10, O15, O25, and O35) and secondary hydroxyl (O3, O13, O23, O24, O28, and O34) groups (Fig. 2c). Moreover, the positional distribution of metal ions around each β-CD molecule is roughly a triangular prism in shape,

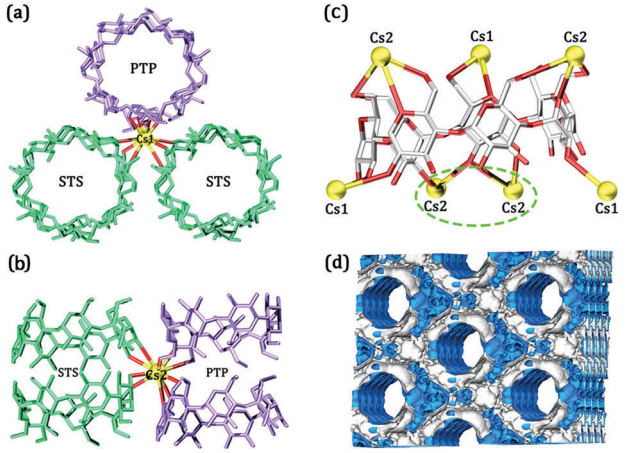

Fig. 2 (a) View of three pairs of β-CD molecules tightly immobilized to the individual Cs1 ion, and each pair stacks in a primary face to primary face/secondary face to secondary face (PTP/STS) manner. (b) View of two pairs of β-CD molecules combined with the individual Cs2 ion; they have the reverse packing arrangement (PTP and STS). (c) The seven metal ions concurrently coordinated to every β-CD molecule are roughly in the shape of a triangular prism, using Cs1/Cs2/Cs2–Cs2 as vertices, by coordination to different combinations (**a–g**, **b–c** and **e–f**) of α-1,4-linked glucopyranosyl units. (d) View of the porosity of the three-dimensional (3D) framework configured with a uniform 1D channel for CD-MOF-**2**. Color code: Cs, yellow; O, red; and C, grey. Hydrogen atoms have been eliminated for clarity.

using Cs1/Cs2/Cs2–Cs2 as a vertex (Fig. 2c), by coordinating to different combinations (**a–g**, **b–c** and **e–f**) of α-1,4-linked glucopyranosyl units. As such, β-CD molecules counted on these metal ion vertexes further assemble into a three-dimensional (3D) framework configured with uniform 1D channels (Fig. 2d) which consist of innumerable "cages". This kind of "cage" was defined by two β-CD molecules connected to two Cs1 and two Cs2 ions and performs secondary face to secondary face stacking. These 1D channels filled with "cages" along the *c* axis endow the eventual CD-MOF-**2** with large "gourd-shaped" cavities (1613.4 Å^3, which accounted for 25.3% of the unit cell volume, calculated using PLATON). We believe that such a cavity peculiarity of CD-MOF-**2** could probably be propitious to selectively accommodate a lot of relatively long organic molecules behaving as experimental models/carriers applied in biological systems.

In order to verify if these two compounds configured with accessible porosity and window size can be treated as carriers for drug delivery, experiments concerning the loading and release of drug molecules were separately conducted in ethanol and phosphate buffer solution (pH = 7.4) under the monitoring of UV-vis spectrophotometry (see the ESI†). The porosity and structural integrity of these two CD-MOFs in ethanol were explored by solvent sorption analyses and PXRD profiles (Fig. S7 and S8, ESI†). Fluorouracil (5-FU, 3 × 6 Å) and methotrexate (MTX, 6 × 10 Å) were finally employed as model drug molecules according to the accessible void sizes of the targeted CD-MOFs. The short biological lifetimes and anti-cancer chemotherapy effects of these two kinds of drugs have made them widely used for sustained or controlled drug delivery.[8,15] Typically, in order to load the model drugs completely, the desolvated CD-MOFs were immersed, respectively, in 5-FU and MTX ethanol solutions for 6 days and then washed. The corresponding loading and release capacities of the targeted drugs for the CD-MOFs were evaluated by UV-vis spectrophotometry using calibration curves (Fig. S9–S14, ESI†). Because of the encapsulation of different concentrations of drugs within their pores at the indicated time intervals, the UV-vis absorption curves of the inclusion complexes show an apparent downtrend in contrast to the beginning of the measurement. As shown in Fig. S15a (ESI†), CD-MOF-**1** and CD-MOF-**2** showed a remarkable 5-FU adsorption compared with the β-CD matrix, and the loading contents were measured to be 1.379 g g^{-1}, 1.510 g g^{-1} and 0.448 g g^{-1}, respectively. The drug-loading capacities of the targeted CD-MOFs are higher than the adsorption achieved with mesoporous silica materials[43] and some MOF drug carriers,[5] but for MTX, CD-MOF-**1** showed an inferior adsorption compared to CD-MOF-**2** and a single β-CD matrix, and the loading contents were separately measured to be 0.689 g g^{-1}, 1.217 g g^{-1} and 0.791 g g^{-1} (Fig. S15b, ESI†). This scenario can be attributed to the following reasons: on the one hand, compared with pure β-CD molecules, CD-MOF-**2** exhibits a uniform 1D channel configured with innumerable "cages", which potentially results in a higher drug loading capacity, due to the complete bareness of the cavity of the β-CD molecule. On the other hand, the primary face and secondary face of each β-CD molecule in CD-MOF-**1** are enclosed by the glucopyranosyl residue of other adjacent β-CD molecules, so that the relatively larger MTX molecules are not conducive to being loaded into CD-MOF-**1**. Finally, at the fourth/fifth day (Fig. S15a and b, ESI†), the loading capacities of the targeted drug molecules reached saturation, that is, the drug loading content reached the maximum, which indicates that the adsorption and desorption of the drug reached equilibrium. As the experiment continues, the loading content began to decrease, which probably means the shedding of drugs adsorbed from the surfaces of the CD-MOFs.

The kinetic process of the 5-FU/MTX delivery in simulated body fluid at 37 °C is shown in Fig. S15c and d (ESI†). As we can see, 5-FU exhibits faster metabolism and the cumulative release degree reaches 96.4% within 40 min. By comparison, 5-FU-loaded CD-MOF-**1** (89%) and CD-MOF-**2** (92%) were released within 5 h. It is clear that the CD-MOFs show a slower release rate of 5-FU. At the same time, the cumulative release rates of MTX were 41.5% for CD-MOF-**1** and 82.4% for CD-MOF-**2**. Compared with CD-MOF-**2**, CD-MOF-**1** with a smaller pore size performed as a more favourable drug-delivery carrier due to its specific channel features, which reveals that the drug delivery in CD-MOFs is directly related to the pore size and the geometry.

In order to evaluate the likelihood and anti-cancer activities of the targeted CD-MOFs as biocompatible drug carriers, we performed *in vitro* cytotoxicity assays whose experimental details are provided in the ESI.† The nontoxic nature of title CD-MOFs was clearly confirmed by the corresponding cytotoxicity results of HepG2 (human hepatoblastoma) cells (Fig. S16, ESI†), and 5-FU/MTX-loaded CD-MOFs with the increased concentration dosages (6.25, 12.5, 25, 50, and 100 μg ml^{-1}) used in this assay showed overall higher HepG2 cell survival rates than those of

5-FU/MTX drug molecules, which can be seen from the optical density (OD) values, as shown in Tables S5 and S6 (ESI†). Within the cytotoxicity tests, 5-FU-CD-MOF-**1** exhibits a lower inhibitory effect on HepG2 cells compared with 5-FU-CD-MOF-**2**, while this order is opposite in the case of MTX-loaded CD-MOFs. The reason for these results is probably due to the discrepant releasing processes, which, respectively, are related to different drug molecules (5-FU/MTX) accommodated into the targeted CD-MOFs. In addition, the combined 50% lethal concentration (IC50) values against HepG2 cells within these cytotoxicity assays also confirmed this trend (Table S7, ESI†), suggesting the biological potential of both of the title CD-MOFs being used as drug carriers.

In summary, for the first time, we have constructed two extremely rare β-CD based MOFs with different porosity characters *via* a template-induced approach. The corresponding investigation of the quantities of control experiments confirmed that the selected template agent plays an important role in changing the crystallinity and porosity of the resulting CD-MOF. We believe that this strategy can be further extended to the development of more CD-MOFs, which may be used in pharmaceutical applications in the future. Moreover, this work also represents the rare use of β-CD based MOFs in controlled drug delivery, which indicates their favourable potential of being used as effective drug carriers.

This work was financially supported by NNSF (No. 21271089), the Talent Culturing Plan for Leading Disciplines of the University in Shandong Province, NNSF (No. 21622104, 21371099 and 21471080), and the NSF of Jiangsu Province of China (No. BK20141445).

Notes and references

1 J.-R. Li, R. J. Kuppler and H.-C. Zhou, *Chem. Soc. Rev.*, 2009, **38**, 1477–1504.
2 A. Dhakshinamoorthy, A. M. Asiri and H. García, *Angew. Chem., Int. Ed.*, 2016, **55**, 5414–5445.
3 L. E. Kreno, K. Leong, O. K. Farha, M. Allendorf, R. P. Van Duyne and J. T. Hupp, *Chem. Rev.*, 2012, **112**, 1105–1125.
4 N. T. T. Nguyen, H. Furukawa, F. Gándara, C. A. Trickett, H. M. Jeong, K. E. Cordova and O. M. Yaghi, *J. Am. Chem. Soc.*, 2015, **137**, 15394–15397.
5 P. Horcajada, R. Gref, T. Baati, P. K. Allan, G. Maurin, P. Couvreur, G. Férey, R. E. Morris and C. Serre, *Chem. Rev.*, 2012, **112**, 1232–1268.
6 P. Horcajada, C. Serre, G. Maurin, N. A. Ramsahye, F. Balas, M. Vallet-Regí, M. Sebban, F. Taulelle and G. Férey, *J. Am. Chem. Soc.*, 2008, **130**, 6774–6780.
7 M. C. Bernini, D. Fairen-Jimenez, M. Pasinetti, A. J. Ramirez-Pastor and R. Q. Snurr, *J. Mater. Chem. B*, 2014, **2**, 766–774.
8 P. P. Bag, D. Wang, Z. Chen and R. Cao, *Chem. Commun.*, 2016, **52**, 3669–3672.
9 Y.-B. Dong, Y.-A. Li, X.-D. Zhao, H.-P. Yin, G. Chen and S. Yang, *Chem. Commun.*, 2016, **52**, 14113–14116.
10 R. A. Smaldone, R. S. Forgan, H. Furukawa, J. J. Gassensmith, A. M. Z. Slawin, O. M. Yaghi and J. F. Stoddart, *Angew. Chem., Int. Ed.*, 2010, **49**, 8630–8634.
11 G. Chen and M. Jiang, *Chem. Soc. Rev.*, 2011, **40**, 2254–2266.
12 J. Szejtli, *J. Mater. Chem.*, 1997, **7**, 575–587.
13 A. R. Hedges, *Chem. Rev.*, 1998, **98**, 2035–2044.
14 S. Han, Y. Wei and B. A. Grzybowski, *Chem. – Eur. J.*, 2013, **19**, 11194–11198.
15 H. J. Lu, X. N. Yang, S. X. Li, Y. Zhang, J. Q. Sha, C. D. Li and J. W. Sun, *Inorg. Chem. Commun.*, 2015, **61**, 48–52.
16 R. S. Forgan, R. A. Smaldone, J. J. Gassensmith, H. Furukawa, D. B. Cordes, Q. Li, C. E. Wilmer, Y. Y. Botros, R. Q. Snurr, A. M. Z. Slawin and J. F. Stoddart, *J. Am. Chem. Soc.*, 2012, **134**, 406–417.
17 J. J. Gassensmith, H. Furukawa, R. A. Smaldone, R. S. Forgan, Y. Y. Botros, O. M. Yaghi and J. F. Stoddart, *J. Am. Chem. Soc.*, 2011, **133**, 15312–15315.
18 Y. Furukawa, T. Ishiwata, K. Sugikawa, K. Kokado and K. Sada, *Angew. Chem., Int. Ed.*, 2012, **51**, 10566–10569.
19 Y. Wei, S. Han, D. A. Walker, P. E. Fuller and B. A. Grzybowski, *Angew. Chem., Int. Ed.*, 2012, **51**, 7435–7439.
20 M. W. Tibbitt, J. E. Dahlman and R. Langer, *J. Am. Chem. Soc.*, 2016, **138**, 704–717.
21 K. T. Holman, *Angew. Chem., Int. Ed.*, 2011, **50**, 1228–1230.
22 K. J. Hartlieb, J. M. Holcroft, P. Z. Moghadam, N. A. Vermeulen, M. M. Algaradah, M. S. Nassar, Y. Y. Botros, R. Q. Snurr and J. F. Stoddart, *J. Am. Chem. Soc.*, 2016, **138**, 2292–2301.
23 V. T. D'Souza and M. L. Bender, *Acc. Chem. Res.*, 1987, **20**, 146–152.
24 I. Nicolis, A. W. Coleman, P. Charpin and C. d. Rango, *Acta Crystallogr., Sect. B: Struct. Sci.*, 1996, **52**, 122–130.
25 F. Cramer, *Angew. Chem.*, 1952, **64**, 136.
26 K. Benner, P. Klüfers and J. Schuhmacher, *Angew. Chem., Int. Ed.*, 1997, **36**, 743–745.
27 R. Fuchs, N. Habermann and P. Klüfers, *Angew. Chem., Int. Ed.*, 1993, **32**, 852–854.
28 P. Klüfers and J. Schuhmacher, *Angew. Chem., Int. Ed.*, 1994, **33**, 1863–1865.
29 I. Nicolis, A. W. Coleman, P. Charpin and C. de Rango, *Angew. Chem., Int. Ed.*, 1995, **34**, 2381–2383.
30 W. Saenger, *Angew. Chem., Int. Ed.*, 1980, **19**, 344–362.
31 K. A. Connors, *Chem. Rev.*, 1997, **97**, 1325–1358.
32 R. Breslow, *Chem. Soc. Rev.*, 1972, **1**, 553–580.
33 P. Klüfers, H. Piotrowski and J. Uhlendorf, *Chem. – Eur. J.*, 1997, **3**, 601–608.
34 M. R. Caira, V. J. Griffith and L. R. Nassimbeni, *J. Inclusion Phenom. Mol. Recognit. Chem.*, 1998, **32**, 461–476.
35 M. Noltemeyer and W. Saenger, *J. Am. Chem. Soc.*, 1980, **102**, 2710–2722.
36 P. A. Chetcuti, P. Moser and G. Rihs, *Organometallics*, 1991, **10**, 2895–2897.
37 K. Benner, J. Ihringer, P. Klüfers and D. Marinov, *Angew. Chem., Int. Ed.*, 2006, **45**, 5818–5822.
38 I. Lippold, H. Görls and W. Plass, *Eur. J. Inorg. Chem.*, 2007, 1487–1491.
39 I. Lippold, K. Vlay, H. Görls and W. Plass, *J. Inorg. Biochem.*, 2009, **103**, 480–486.
40 I. Nicolis, A. W. Coleman, M. Selkti, F. Villain, P. Charpin and C. de Rango, *J. Phys. Org. Chem.*, 2001, **14**, 35–37.
41 Y. X. Li, W. Zhang, Z. Liu and Z. G. Xie, *Acta Chim. Sin.*, 2015, **73**, 641–645.
42 W. Michida, M. Ezaki, M. Sakuragi, G. Q. Guan and K. Kusakabe, *Cryst. Res. Technol.*, 2015, **50**, 556–559.
43 F. Qu, G. Zhu, H. Lin, W. Zhang, J. Sun, S. Li and S. Qiu, *J. Solid State Chem.*, 2006, **179**, 2027–2035.